

$$[\text{OH}^*] = ((([\text{TiO}_2^-]k_{rc})^2 + 4k_t I_0 \phi_0)^{1/2} - [\text{TiO}_2^-]k_{rc}) / 2k_t \quad (21)$$

and

$$dP/dt = [\text{OH}^*]k_p P = \frac{((( [\text{TiO}_2^-]k_{rc})^2 + 4k_t I_0 \phi_0 )^{1/2} - [\text{TiO}_2^-]k_{rc})k_p P}{2k_t} \quad (22)$$

Thus, the dependence of the pseudo-first-order reaction rate  $[\text{OH}^*]k_p$  on light intensity is a function of the relative magnitude of the light intensity relative to  $([\text{TiO}_2^-]k_{rc})^2$ . At high light intensity, we would see a square root dependence, while at low intensity, we would see a linear dependence.

Such behavior of rate on light intensity has been observed in several laboratories<sup>4,51</sup> and in one case<sup>4</sup> attributed to recombination processes. Our proposed mechanism allows for a square root

dependence in a more general scheme.

### Conclusions

We have proposed a mechanism that describes the photoresponse of a  $\text{TiO}_2$  slurry in a PEC slurry cell. This mechanism accounts for previously observed results on photodetoxification with  $\text{TiO}_2$  involving addition of  $\text{H}_2\text{O}_2$  where both increases and decreases in the rate of pollutant decomposition can be observed. We demonstrate that for pollutant decomposition by  $\text{OH}^*$  the pseudo-first-order disappearance of pollutant will vary as  $I_0^{1/2}$  for high light intensity and be linear in light intensity at low intensity. Finally we note that eqs 3, 12, and 13 represent fundamental limitations on any system that relies on  $\text{OH}^*$  as the primary mode of hole transfer to the pollutant.

*Acknowledgment.* This work was supported by the U.S. Department of Energy, Office of Conservation and Renewable Energy, Solar Thermal Program.

(51) Kormann, C. Ph.D. Thesis, California Institute of Technology, Pasadena, CA, 1989.

## Cationic Trirhenium Rafts on $\gamma\text{-Al}_2\text{O}_3$ : Characterization by X-ray Absorption Spectroscopy

A. S. Fung,<sup>†</sup> P. A. Tooley,<sup>†</sup> M. J. Kelley,<sup>†</sup> D. C. Koningsberger,<sup>§</sup> and B. C. Gates<sup>\*†</sup>

*Center for Catalytic Science and Technology, Department of Chemical Engineering, University of Delaware, Newark, Delaware 19716; Engineering Technology Laboratory, Experimental Station, E. I. duPont deNemours and Co., Wilmington, Delaware 19898; and Department of Inorganic Chemistry and Catalysis, Eindhoven University of Technology, P.O. Box 513, 5600 MB Eindhoven, The Netherlands (Received: January 26, 1990; In Final Form: July 3, 1990)*

Rhenium surface species, derived by treating  $[\text{H}_3\text{Re}_3(\text{CO})_{12}]$  adsorbed on  $\gamma\text{-Al}_2\text{O}_3$  in hydrogen at 400 °C, formed extremely small surface grouping of rhenium atoms having an average Re-Re coordination number of 2, as determined by extended X-ray absorption fine structure (EXAFS) spectroscopy. Results of X-ray photoelectron spectroscopy and threshold resonance experiments show that the rhenium was cationic, with oxidation states of about +4 to +6. Infrared spectroscopy was used to follow the decomposition of surface species derived from  $[\text{H}_3\text{Re}_3(\text{CO})_{12}]$  adsorbed on  $\gamma\text{-Al}_2\text{O}_3$ , the data indicating that Re subcarbonyls such as  $[\text{Re}(\text{CO})_3\{\text{O}-\text{Al}\}_2\{\text{HO}-\text{Al}\}]$  were formed as intermediates. On the basis of the Re-O and Re-Re coordination parameters determined by EXAFS spectroscopy, a structural model of cationic trirhenium rafts on the  $\gamma\text{-Al}_2\text{O}_3$  surface is suggested. This structure is characterized by a Re-Re distance of 2.67 Å, which is greater than the distances characterizing the quadruple and triple Re bonds (2.3 Å) in Re complexes but shorter than the distance in bulk metallic Re (2.74 Å). The Re-Re distance suggests an intermediate bond order, roughly 1.5. The trirhenium rafts are suggested to be tethered to surface oxygens with a Re-O distance of 2.05 Å indicated by the EXAFS data. A longer Re-O distance, 2.58 Å, is also indicated by the EXAFS data, and this is suggested to be indicative of interactions of the rhenium with surface hydroxyl groups. Another  $\gamma\text{-Al}_2\text{O}_3$ -supported Re sample was prepared by a conventional method with aqueous  $\text{NH}_4\text{ReO}_4$  as the precursor, with treatment in hydrogen at 450 °C. The resulting surface species were highly nonuniform, consisting of surface rhenium oxide species and metallic rhenium particles.

### Introduction

Technological materials ranging from highly dispersed supported metal catalysts to microelectronic devices incorporate metal microstructures on metal oxide supports. The structures of these metal microstructures and the interfaces between them and metal oxide supports are less than well defined because the metal entities are extremely small and nonuniform. One of the most powerful techniques for understanding such structures is X-ray absorption spectroscopy,<sup>1</sup> especially extended X-ray absorption fine structure (EXAFS) spectroscopy. The goal of this research was to synthesize extremely small and structurally uniform metal entities on the surface of a metal oxide and to determine the structure in detail, with a focus on the metal-support interface. The metal was chosen to be Re because Re cations are oxophilic, bonding

strongly to metal oxide surfaces.

Yao and Shelef<sup>2</sup> reported temperature-programmed desorption, electron spin resonance spectroscopy, and chemisorption measurements indicating that Re on  $\gamma\text{-Al}_2\text{O}_3$  was present as highly dispersed two-dimensional rafts in addition to a crystalline three-dimensional phase. Raman spectra also gave evidence of monolayer raftlike structures of Re on  $\gamma\text{-Al}_2\text{O}_3$ .<sup>3</sup> The existence of these rafts was questioned by Arnoldy et al.,<sup>4</sup> who attributed a high-temperature peak in the temperature-programmed-reduction spectrum to carbonaceous impurities in the sample rather

(1) Koningsberger, D. C.; Prins, R. *X-ray Absorption: Principles, Applications, Techniques of EXAFS, SEXAFS and XANES*; Wiley: New York, 1988.

(2) Yao, H. C.; Shelef, M. *J. Catal.* **1976**, *44*, 392.

(3) Hardcastle, F. D.; Wachs, I. E.; Horsley, J. A.; Via, G. H. *J. Mol. Catal.* **1988**, *46*, 15.

(4) Arnoldy, P.; van Oers, E. M.; Bruinsma, O. S. L.; de Beer, V. H. J.; Mouljn, J. A. *J. Catal.* **1985**, *93*, 231.

<sup>†</sup> University of Delaware.

<sup>\*</sup> E. I. duPont deNemours and Co.

<sup>§</sup> Eindhoven University of Technology.

than to a difficult-to-reduce monolayer of Re.

Other metals (including Pt,<sup>5</sup> Rh,<sup>6,7</sup> Ru,<sup>8</sup> Os,<sup>8</sup> W,<sup>9</sup> and Ir<sup>10</sup> on metal oxide supports have been inferred to exist in the form of monolayer rafts, with the structural evidence including transmission electron microscopy and CO chemisorption measurements. Perhaps the best-defined raftlike structures are those formed from [Ir<sub>4</sub>(CO)<sub>12</sub>] on  $\gamma$ -Al<sub>2</sub>O<sub>3</sub>,<sup>10,11</sup> which have been characterized by EXAFS spectroscopy. The data are consistent with an Ir raft structure, but they also indicate the presence of a high concentration of low-atomic-weight backscatterers consistent with the presence of a carbon overlayer stabilizing the metal layer. Since highly dispersed metals on supports may be oxidized and fragmented by exposure to CO,<sup>12-14</sup> there is still some question about the existence of rafts in most of these samples.

A goal of this research was to form  $\gamma$ -Al<sub>2</sub>O<sub>3</sub>-supported Re rafts from trinuclear organorhenium clusters, [H<sub>3</sub>Re<sub>3</sub>(CO)<sub>12</sub>], chosen to minimize impurities (such as chloride) that would be retained on the support surface and maximizing the likelihood of formation of highly dispersed structures. It was hoped that trinuclear Re units would be retained on the surface. EXAFS spectroscopy was used to characterize the metal and the metal-metal oxide interface, and X-ray photoelectron spectroscopy and X-ray absorption near-edge structure (XANES) measurements were used to estimate the oxidation state of the Re. For comparison, samples were also made from NH<sub>4</sub>ReO<sub>4</sub> by the conventional incipient wetness technique used to make supported rhenium catalysts.

### Experimental Methods

**Sample Preparation and Handling.** Sample preparation and handling were performed under dry nitrogen in a Vacuum Atmospheres drybox, on a double manifold Schlenk line, and in nitrogen-filled transfer vessels. [Re<sub>2</sub>(CO)<sub>10</sub>] (Strem) and NH<sub>4</sub>ReO<sub>4</sub> (Alfa) were used without purification. Hexanes and cyclohexane were reagent grade and were dried by distilling from sodium benzophenone ketyl. Hydrogen with a purity of 99.999% was purchased from Matheson. It was passed through beds of activated 4A molecular sieves and Cu<sub>2</sub>O to remove traces of moisture and oxygen. [H<sub>3</sub>Re<sub>3</sub>(CO)<sub>12</sub>]<sup>15</sup> and [Re(CO)<sub>3</sub>OH]<sub>4</sub><sup>16</sup> were synthesized by the literature methods.

The  $\gamma$ -Al<sub>2</sub>O<sub>3</sub> support (Degussa, Aluminum Oxid C) was made into a paste by adding deionized distilled water, followed by drying at 120 °C overnight. It was ground and then calcined at 500 °C for 2 h and evacuated (pressure <10<sup>-3</sup> Torr) at 500 °C overnight. The partially dehydroxylated support material had a BET surface area of 104 m<sup>2</sup>/g and was stored in the drybox before use.

In a standard preparation, [H<sub>3</sub>Re<sub>3</sub>(CO)<sub>12</sub>] was brought in contact with pretreated  $\gamma$ -Al<sub>2</sub>O<sub>3</sub> by slurring in freshly distilled hexanes for 4 h. The solvent was then pumped off and the solid dried in vacuo overnight. The sample was stored under dry nitrogen. Another Re-on-alumina sample was synthesized by the incipient wetness technique with an aqueous solution of NH<sub>4</sub>ReO<sub>4</sub> made from doubly distilled deionized water. The sample was calcined at 500 °C in flowing air for 2 h followed by heating in flowing N<sub>2</sub> (99.99% purity) at 500 °C for 2 h to attain a better

dispersion after reduction.<sup>2</sup> The Re loadings of the [H<sub>3</sub>Re<sub>3</sub>(CO)<sub>12</sub>]-derived and NH<sub>4</sub>ReO<sub>4</sub>-derived samples were 1.2 and 1.0 wt %, respectively, as determined by X-ray fluorescence spectroscopy with a Philips PW 1410/80 automated X-ray spectrometer.

**Infrared Spectroscopy.** Infrared spectra were measured with a Nicolet 7199 Fourier transform infrared spectrometer with a spectral resolution of 2 cm<sup>-1</sup>. Solution spectra were obtained with a 0.2-mm CaF<sub>2</sub> cell. Solid samples were pressed at a pressure of 6.9 × 10<sup>7</sup> Pa into self-supporting thin wafers and characterized in a controlled-environment quartz cell with NaCl windows.<sup>17</sup> The infrared cell was interfaced to a gas manifold so that the sample could be treated in gaseous environments or under vacuum.

The structural evolution of the surface species derived from adsorbing organometallic precursors on partially dehydroxylated  $\gamma$ -Al<sub>2</sub>O<sub>3</sub> under hydrogen was monitored by measuring the infrared absorption in the carbonyl region. Each sample was heated from ambient temperature to 400 °C in 50 °C intervals and then treated in hydrogen at 400 °C for 4 h.

**X-ray Photoelectron Spectroscopy.** The experiments were carried out with a Physical Electronics AES/XPS spectrometer (Model 551) equipped with an AlK $\alpha$  anode (10 kV, 60 mA, 1486.6 eV) and a cylindrical mirror analyzer. The base pressure in the vacuum chamber was always <5 × 10<sup>-9</sup> Torr, with typical operating pressures <5 × 10<sup>-8</sup> Torr. Samples were ground and mounted as powders by packing into aluminum holders with 1 cm diameter × 1 mm deep cavities using an aluminum hand press. The sample was attached to a heatable sample-transfer probe with screws and copper clips. Samples were transferred from the drybox to the prechamber of the spectrometer under a nitrogen blanket enclosed in a 2-gal plastic bag. The prechamber was connected to a turbomolecular pump and a gas manifold so that the samples could be subjected to in situ gas treatments and evacuation.

In a typical experiment, an alumina-supported sample prepared from [H<sub>3</sub>Re<sub>3</sub>(CO)<sub>12</sub>] was first evacuated at room temperature in the prechamber to remove traces of physisorbed water. It was then treated in flowing hydrogen at 400 °C for 2 h (flow rate, 100 mL/min; heating rate, 5 °C/min). After cooling to room temperature, the prechamber was evacuated to a pressure <10<sup>-6</sup> Torr and the sample introduced into the ultra-high-vacuum chamber. Data were collected overnight. The C 1s binding energy (284.6 eV) was used as a reference to determine the binding energies of the reference compounds. The Al 2p binding energy (74.5 eV) was used as the internal reference, and the C 1s binding energy was used to check the internal consistency of the binding energy assignments. Re foil (the surface oxide layer was removed by Ar<sup>+</sup> sputtering), [Re(CO)<sub>3</sub>OH]<sub>4</sub>,<sup>16</sup> ReO<sub>2</sub> (Strem), and Re<sub>2</sub>O<sub>7</sub> (Strem) were used to characterize the binding energies of Re(0), Re(I), Re(IV), and Re(VII), respectively. To avoid the decomposition of [Re(CO)<sub>3</sub>OH]<sub>4</sub>, it was mounted on indium foil and cooled to liquid-nitrogen temperature during data acquisition.

**X-ray Absorption Spectroscopy.** Each sample was pressed to give a self-supporting wafer in a sample holder, with the amount calculated to yield optimal absorption measurements at the Re L<sub>III</sub> edge (total absorbance  $\mu x = 2.5$ , fractional absorbance by Re  $\cong 0.3$ ). The sample holder was mounted in a heatable and evacuable in situ EXAFS cell equipped with thin Be windows.<sup>18,19</sup> Sample treatment at high temperature and transmission measurements at liquid-nitrogen temperature were performed with the sample in the same cell, protected from exposure to air.

The alumina-supported sample prepared from [H<sub>3</sub>Re<sub>3</sub>(CO)<sub>12</sub>] was treated in flowing hydrogen (99.999% purity, 100 mL/min) while being heated at a rate of 5 °C/min to 400 °C. After treatment at 400 °C for 4 h, the sample was cooled to room temperature under flowing hydrogen, and data were collected with the sample under static hydrogen after cooling to approximately liquid-nitrogen temperature. The alumina-supported sample

(5) Spenadel, L.; Boudart, M. *J. Phys. Chem.* **1960**, *64*, 204.

(6) Prestridge, E. B.; Yates, D. J. C. *Nature* **1971**, *234*, 345.

(7) Yates, D. J. C.; Murrell, L. L.; Prestridge, E. B. *J. Catal.* **1979**, *57*, 41.

(8) Prestridge, E. B.; Via, G. H.; Sinfelt, J. H. *J. Catal.* **1977**, *50*, 115.

(9) Chan, S. S.; Wachs, I. E.; Murrell, L. L.; Dispenziere, N. C., Jr. *J. Catal.* **1985**, *92*, 1.

(10) van Zon, F. B. M.; Koningsberger, D. C. *Proceedings of the 9th International Congress on Catalysis*; Phillips, M. J., Ternan, M., Eds.; Chemical Institute of Canada: Ottawa, 1988; Vol. III, p 1386.

(11) van Zon, F. B. M. Ph.D. Dissertation, Eindhoven University of Technology, 1988.

(12) Primet, M. *J. Chem. Soc., Faraday Trans. 1* **1978**, *74*, 2570.

(13) van't Blik, H. F. J.; van Zon, J. B. A. D.; Huizinga, T.; Vis, J. C.; Koningsberger, D. C.; Prins, R. *J. Am. Chem. Soc.* **1985**, *107*, 3139.

(14) Basu, P.; Panayotov, D.; Yates, J. T. *J. Am. Chem. Soc.* **1988**, *110*, 2074.

(15) Andrews, M. A.; Kirtley, S. W.; Kaesz, H. D. *Inorg. Synth.* **1977**, *17*, 16.

(16) Herberhold, M.; Suss, G.; Ellerman, J.; Gabelein, H. *Chem. Ber.* **1978**, *111*, 2931.

(17) Barth, R.; Gates, B. C.; Zhao, Y.; Knözinger, H.; Hulse, J. *J. Catal.* **1983**, *82*, 147.

(18) Lornston, J. M. Ph.D. Dissertation, University of Delaware, 1980.

(19) Kampers, F. W. H.; van Grondelle, J.; Brinkgreve, P.; Koningsberger, D. C. *Rev. Sci. Instrum.*, in press.

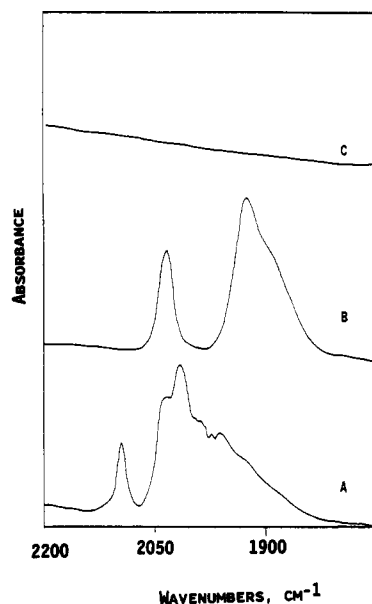


**Figure 1.** Infrared spectra in the carbonyl region of (A) sample prepared by adsorption of  $[\text{H}_3\text{Re}_3(\text{CO})_{12}]$  from hexanes onto  $\gamma$ -Al<sub>2</sub>O<sub>3</sub> under N<sub>2</sub>; (B) after 0.5 h of exposure to H<sub>2</sub> at 1 atm and 150 °C; (C) after 2 h of exposure to H<sub>2</sub> at 1 atm and 400 °C.

derived from NH<sub>4</sub>ReO<sub>4</sub> was first dried in He for 1 h at 450 °C followed by treatment in flowing hydrogen for 4 h at 450 °C. Data were collected under the same conditions mentioned above.

Reference compounds were also characterized by X-ray absorption spectroscopy and the reference data used for analysis of the data obtained for the supported Re samples. The measurements were made at liquid-nitrogen temperature. Re powder (average particle size, 3–4  $\mu\text{m}$ , 99.99% purity, Goodfellow) was physically mixed with  $\gamma$ -Al<sub>2</sub>O<sub>3</sub> and pressed into a self-supporting wafer. The sample in the EXAFS cell was treated in flowing hydrogen at 400 °C for 1 h and cooled in flowing hydrogen. The other reference compound, NH<sub>4</sub>ReO<sub>4</sub> (Alfa), was used as supplied; the powder samples were mixed with  $\gamma$ -Al<sub>2</sub>O<sub>3</sub> to achieve an optimal Re absorption of  $\Delta\mu x = 1$ .

X-ray absorption spectra were measured at beamline X-11-A of the National Synchrotron Light Source at Brookhaven National Laboratory (2.5 GeV, 60–145 mA) with a Si(111) monochromator. Data were also collected at the wiggler station 9.2 at the Synchrotron Radiation Source of Daresbury Laboratory, U.K. (1.9 GeV, 100–200 mA), with a Si(220) monochromator. All experiments were performed with the monochromator detuned at 50% to minimize contaminations that arise from higher harmonics. Measurements were done at the Re L<sub>III</sub> edge (10534 eV).

The internal consistency of results obtained at the different stations was always checked with EXAFS data collected with a standard 3.5- $\mu\text{m}$  Pt foil; differences in amplitude were no more than 10% from one data set to another. Precautions were taken to optimize all the EXAFS spectrometers and data collecting procedures to maximize the signal to noise ratio.<sup>20</sup>

## Results

**Infrared Spectroscopy.** The formation of rhenium surface species derived from the supported cluster was characterized by in situ infrared spectroscopy. A sample prepared from  $[\text{H}_3\text{Re}_3(\text{CO})_{12}]$  adsorbed on alumina was treated in hydrogen at 150 °C for 0.5 h. The infrared absorption band pattern (2037 (s), 1925 (s), and 1895 (sh) cm<sup>-1</sup>) is in close agreement with that characteristic of a mononuclear rhenium subcarbonyl species having C<sub>s</sub> symmetry, as observed by Kirilin et al.<sup>21</sup> (Figure 1B).

(20) Sayers, D. E.; Bunker, B. A. In *X-ray Absorption: Principles, Applications, Techniques of EXAFS, SEXAFS and XANES*; Koningsberger, D. C., Prins, R., Eds.; Wiley: New York, 1988; Chapter 6.

(21) Kirilin, P. S.; DeThomas, F. A.; Bailey, J. W.; Gold, H. S.; Dybowski, C.; Gates, B. C. *J. Phys. Chem.* **1986**, *90*, 4882.

**TABLE I: XPS Data: Binding Energies of Re Reference Compounds and the Sample Prepared from  $[\text{H}_3\text{Re}_3(\text{CO})_{12}]$ <sup>24</sup>**

sample	BE, eV	
	Re 4f <sub>7/2</sub>	C 1s <sup>a</sup>
reference compd		
Re foil	40.0	(284.6)
$[\text{Re}(\text{OH})(\text{CO})_3]_4$	40.2	(284.6)
ReO <sub>2</sub>	42.5	(284.6)
Re <sub>2</sub> O <sub>7</sub>	46.4	(284.6)
precursor/support		
$[\text{H}_3\text{Re}_3(\text{CO})_{12}]/\text{Al}_2\text{O}_3$ <sup>b</sup>	46.7	284.6

<sup>a</sup>C 1s = 284.6 eV is used as the reference binding energy for the reference compounds and is in parentheses. <sup>b</sup>Sample treatment: H<sub>2</sub> preheat, H<sub>2</sub> reduction at 400 °C, 2 h.

**TABLE II: XPS Data: Re 4f<sub>7/2</sub> Binding Energies of Re Reference Compounds**

reference compound							
Re		ReO		ReO <sub>2</sub>		Re <sub>2</sub> O <sub>7</sub>	
BE, eV	ref	BE, eV	ref	BE, eV	ref	BE, eV	ref
40.6 <sup>a</sup>	25			43.2 <sup>a</sup>	25	46.5 <sup>a</sup>	25
40.2 <sup>b</sup>	26	41.6 <sup>b</sup>	26	43.1 <sup>b</sup>	26	46.4 <sup>b</sup>	26
40.1 <sup>a</sup>	27			42.5 <sup>a</sup>	27	46.9 <sup>a</sup>	27
39.7 <sup>c</sup>	28	41.3 <sup>c</sup>	28	42.5 <sup>c</sup>	28	46.7 <sup>c</sup>	28

<sup>a</sup>Reference binding energy, C 1s = 285 eV. <sup>b</sup>Reference binding energy, C 1s = 284.6 eV. <sup>c</sup>Reference binding energy, Pt 4f<sub>7/2</sub> = 70.9 eV.

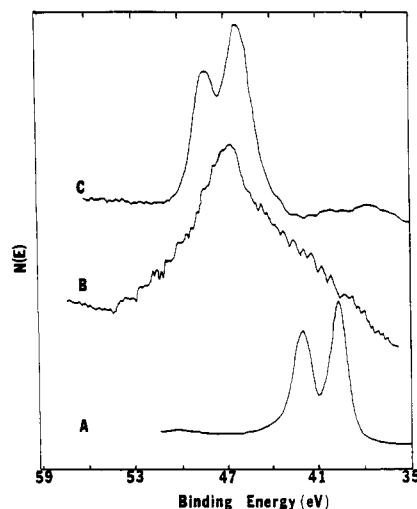


**Figure 2.** XP spectra of (A) Re foil, (B) the sample prepared from  $[\text{H}_3\text{Re}_3(\text{CO})_{12}]$  after treatment in H<sub>2</sub> at 400 °C for 2 h, and (C) Re<sub>2</sub>O<sub>7</sub>.

Evidently, the supported Re cluster had been disrupted upon heating, resulting in the formation of the partially oxidized rhenium subcarbonyl species. This rhenium subcarbonyl species is formulated as  $[\text{Re}(\text{CO})_3\{\text{O}-\text{Al}\}_2\{\text{HO}-\text{Al}\}]$  and has been examined by Kirilin et al. with vibrational spectroscopies.<sup>21</sup> The MgO-supported analogue has been characterized by X-ray absorption (EXAFS) spectroscopy.<sup>22</sup> (Kirilin et al. initially formulated the surface species as  $[\text{Re}(\text{CO})_3\{\text{O}-\text{Al}\}\{\text{HO}-\text{Al}\}_2]$ , but more recent results for the MgO-supported analogue suggest that the former formulation is a better approximation.<sup>23</sup>) After 2 h of treatment

(22) Kirilin, P. S.; van Zon, F. B. M.; Koningsberger, D. C.; Gates, B. C. *J. Phys. Chem.* **1990**, *94*, 8439.

(23) Papile, C. J.; Gates, B. C. To be published.

(24) Kelley, M. J.; Fung, A. S.; McDevitt, M. R.; Tooley, P. A.; Gates, B. C. In *Microstructures and Properties of Catalysts*; MRS Proc. Vol. III; Treacy, M. M. J., White, J. M., Thomas, J. M., Eds.; Materials Research Society: Pittsburgh, PA, 1988.

(25) Shpiro, E. S.; Avaev, V. I.; Antoshin, G. V.; Ryashentseva, M. A.; Minachev, Kh. M. *J. Catal.* **1978**, *55*, 402.

(26) Nguyen, H. H.; Salvati, L.; Hercules, D. M. To be published.

(27) Cimino, A.; Deangelis, B. A.; Gazzoli, D.; Valigi, M. *Z. Inorg. Allg. Chem.* **1980**, *460*, 86.

(28) Tysoe, W. T.; Zaera, F.; Somorjai, G. A. *Surf. Sci.* **1988**, *200*, 1.

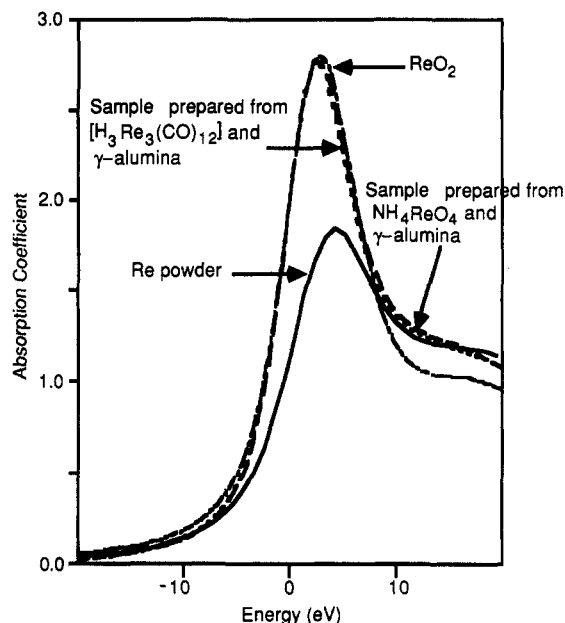


**Figure 3.** A comparison of the Re  $L_{III}$  absorption edges of Re reference compounds, the sample prepared from  $[H_3Re_3(CO)_{12}]$  adsorbed on alumina, and the sample prepared from  $NH_4ReO_4$  adsorbed on alumina.

in  $H_2$  at 400 °C, no infrared absorption was observed in the carbonyl region, indicating that the Re surface species had been completely decarbonylated (Figure 1C).

**Oxidation State of Re in Samples Prepared from Alumina-Supported  $[H_3Re_3(CO)_{12}]$ .** The binding energies of Re in Re foil ( $Ar^+$  sputtered),  $[Re(CO)_3OH]_4$ ,  $ReO_2$ , and  $Re_2O_7$  were measured as references for Re(0), Re(I), Re(IV), and Re(VII), respectively (Table I). The Re  $4f_{7/2}$  binding energy measured for Re(IV) in  $ReO_2$  is 42.5 eV, which is in close agreement with values reported in the literature (Table II). Binding energies corresponding to Re(VII) were also detected in the  $ReO_2$  sample, probably caused by air oxidation leading to the formation of a surface layer of  $Re_2O_7$ .

The large difference in binding energies for Re(0) and Re(VII) (40.0 and 46.4 eV, respectively) (Table I) allows a clear distinction between Re(0) and Re(VII) by XPS, but the method is not sufficient to distinguish Re(0) and Re(I) (40.0 and 40.2 eV) in the supported samples. The XP spectrum of the cluster-derived Re sample after treatment in hydrogen at 400 °C is shown in Figure 2. The peak is broad, with an average binding energy of 46.7 eV, suggesting a mixture of Re surface species with oxidation states in the range of +4 to +6.

Additional results characterizing the chemical states of Re are provided by the X-ray absorption edge data.<sup>29</sup> The intensities of the threshold resonances of the L absorption edges are related to the transition probabilities of exciting inner-core 2p electrons ( $2p_{1/2}$  and  $2p_{3/2}$ ) to the vacant d valence levels. The higher the oxidation state of the metal, the greater the number of vacancies in the valence level, and hence the higher the probability of the transition of the inner-core p electrons to this level. Therefore, a measurement of both the  $L_{II}$  and  $L_{III}$  absorption edges would characterize the oxidation state of the metal.<sup>30,31</sup> Since only the  $L_{III}$  absorption edge was measured, only a qualitative indication of the Re oxidation state is available. The  $L_{III}$  absorption edge data are used only as a fingerprint.<sup>32</sup>

The intensity of the Re  $L_{III}$  threshold resonance of the  $[H_3Re_3(CO)_{12}]$ -derived sample is compared with those measured for  $ReO_2$  and for Re powder that had been treated in  $H_2$  in the

**TABLE III: Crystallographic Data for the Reference Compounds and Fourier Transform Ranges Used in the Isolation of Each for EXAFS Analysis**

reference compd	A-B <sup>a</sup>	R, Å	N <sup>b</sup>	ref	n <sup>c</sup>	Fourier transform	
						k range, Å <sup>-1</sup>	R range, Å
Re powder	Re-Re	2.74	12	34	3	2.86–16.39	1.65–3.38
$NH_4ReO_4$	Re-O	1.74	4	35	3	2.84–13.83	0.80–2.52

<sup>a</sup>A-B: absorber-backscatterer pair. <sup>b</sup>N, coordination number. <sup>c</sup>n, exponent of the weighting factor of Fourier transform.

X-ray absorption cell (Figure 3). The intensity of the threshold resonance of the  $L_{III}$  edge characterizing the sample prepared from  $[H_3Re_3(CO)_{12}]$  adsorbed on alumina after reduction at 400 °C is similar to that observed for  $ReO_2$ . This result is consistent with the XPS results indicating that the cationic Re is present in oxidation states in the range of +4 to +6.

Similarly, the oxidation state of Re of the sample prepared from  $NH_4ReO_4$  on  $\gamma-Al_2O_3$  after treatment in hydrogen at 450 °C is estimated from the intensity of the threshold resonance of the Re  $L_{III}$  absorption edge. The intensity of the absorption edge characterizing the sample is comparable to that of  $ReO_2$ , indicating that Re has an average oxidation state of about +4 after treatment in hydrogen at 450 °C.

**EXAFS Data Analysis. Extraction of the EXAFS Function from Raw Data.** The EXAFS function ( $\chi$ ) was obtained from the experimental X-ray absorption spectrum by subtracting a quadratic expansion based on the extrapolation of the pre-edge region followed by a cubic spline background removal.<sup>33</sup> The derivative of the background and the magnitude of the Fourier transform of the EXAFS function were used as criteria for appropriate background removal. An optimal solution was judged to have been reached when there were few oscillations in the derivative of the background and when the magnitude of the Fourier transform of the EXAFS function between  $R = 0$  and 1 Å ( $R$  is the average distance between the absorbing atom, Re, and the backscattering atom) was at its minimum, without, however, there being a substantial loss in the intensity of the major peak in the spectrum. The resulting EXAFS function was then normalized to the height of the absorption edge and analyzed for structural information.

**Reference Compounds.** The EXAFS data and the Fourier transforms of the data for the reference compounds for each absorber and backscatterer pair are shown in Figure 4. The Fourier transform range ( $k_{min}$  and  $k_{max}$ ;  $k$  is the wavenumber) and the crystallographic data characterizing the first coordination shell of each reference compound are listed in Table III.

**The Supported Re Samples.** The EXAFS data characterizing the  $\gamma-Al_2O_3$ -supported sample prepared from  $[H_3Re_3(CO)_{12}]$  and those characterizing the sample prepared from  $NH_4ReO_4$  after treatment in hydrogen are shown in Figure 5. The latter data show oscillations up to  $k = 16 \text{ Å}^{-1}$ ; these oscillations are weaker in the spectrum characterizing the sample prepared from  $[H_3Re_3(CO)_{12}]$  than in the spectrum of the sample prepared from  $NH_4ReO_4$ . These oscillations at high values of  $k$  can be interpreted as arising from the presence of Re metal crystallites. This result suggests that different structures were present in the two samples, as is confirmed by a comparison of the  $k^3$ -weighted Fourier transforms of the EXAFS data for the two samples.

The experimental EXAFS ( $\chi$ ) data were analyzed by fitting in  $k$  space and in  $r$  (distance) space. The different contributions in the EXAFS data were identified by using phase- and amplitude-corrected Fourier transforms in combination with the difference file technique.<sup>37</sup> Briefly, the EXAFS function of the first coordination shell,  $\chi_1$ , was first obtained by inverse Fourier transformation of the  $\chi$  data. The major contribution in the first

(29) Lytle, F. W.; Wei, P. S. P.; Greeger, R. B.; Via, G. H.; Sinfelt, J. H. *J. Chem. Phys.* **1979**, *70*, 4849.

(30) Horsely, J. A. *J. Chem. Phys.* **1982**, *76*, 1451.

(31) Mansour, A. N.; Cook, J. W.; Sayers, D. E. *J. Phys. Chem.* **1984**, *88*, 2330.

(32) Meitzner, G.; Via, G. H.; Lytle, F. W.; Sinfelt, J. H. *J. Chem. Phys.* **1987**, *87*, 6354.

(33) Cook, J. W. Jr.; Sayers, D. E. *J. Appl. Phys.* **1981**, *52*(8), 5024.

(34) Kittel, C. *Introduction to Solid State Physics*, 6th ed.; Wiley: New York, 1986; p 24.

(35) Brown, R. J. C.; Segel, S. L.; Dolling, G. *Acta Crystallogr.* **1980**, *B36*, 2195.

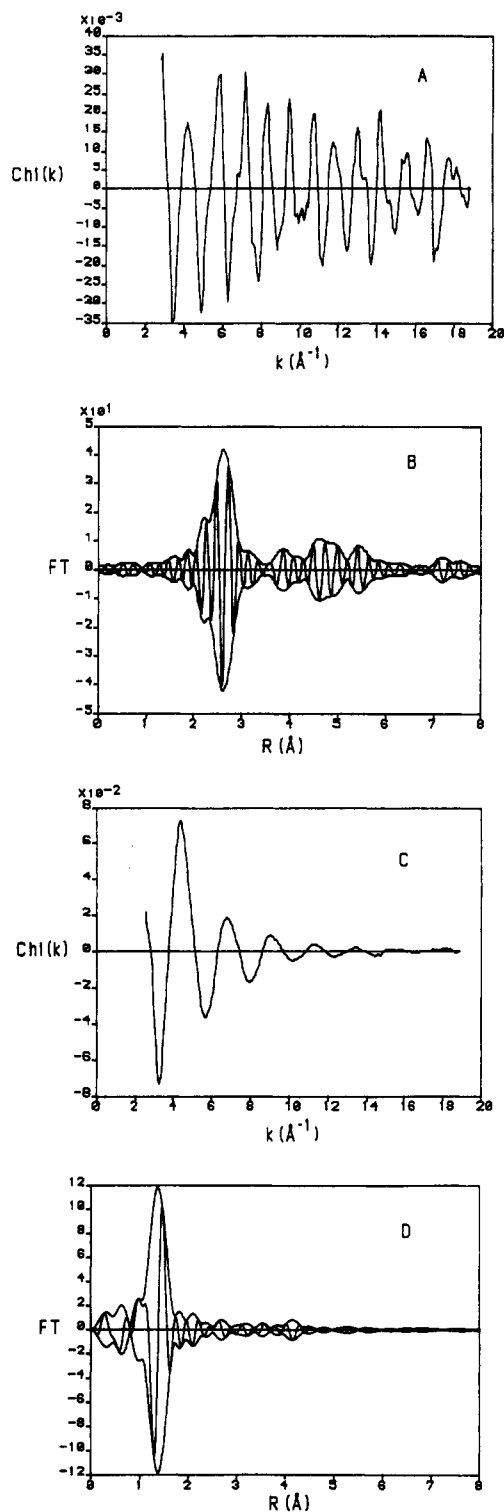


Figure 4. EXAFS spectra of (A) raw  $\chi$  data of Re powder; (B)  $k^3$ -weighted Fourier transform (FT) of the  $\chi$  data characterizing the Re powder; (C) raw  $\chi$  data of  $\text{NH}_4\text{ReO}_4$ ; (D)  $k^3$ -weighted Fourier transform of the  $\chi$  data characterizing the  $\text{NH}_4\text{ReO}_4$ .

shell was then identified by using Fourier transforms with different weightings with various experimentally derived phase-shift functions. As a result, the contributions associated with low- $Z$  (low-atomic-weight) and high- $Z$  backscatters in the magnitude of the Fourier transform could be suitably enhanced or attenuated. The dominant contribution was analyzed first. After the best fit had been obtained, a model calculation of this contribution,  $\chi_{\text{model}}$ , was made on the basis of the phase and amplitude functions of the corresponding reference compound. The resulting calculated  $\chi$  function was then subtracted from the experimental results. The residual EXAFS function,  $\chi_1 - \chi_{\text{model}}$ , was further analyzed for other

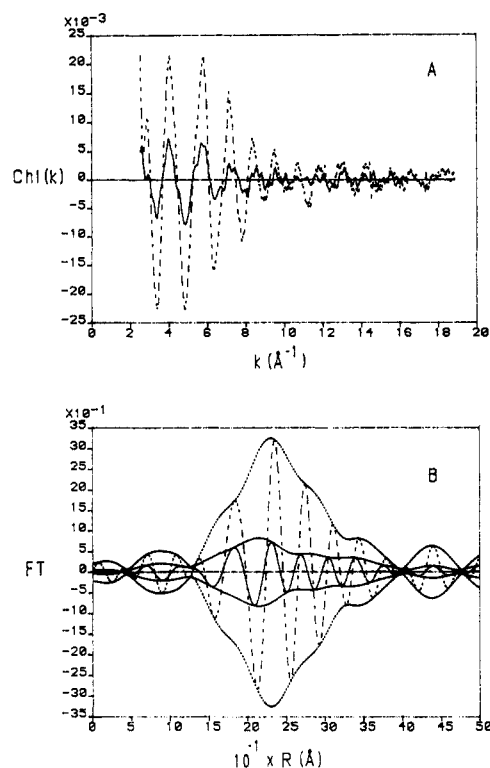


Figure 5. A comparison of (A) the raw  $\chi$  data and (B) the  $k^3$ -weighted Fourier transform ( $\Delta k = 3.05 \times 10 \text{\AA}^{-1}$ ) characterizing the alumina-supported sample prepared from  $[\text{H}_3\text{Re}_3(\text{CO})_{12}]$  (full line) and the sample prepared from  $\text{NH}_4\text{ReO}_4$  (dashed line). In B, the envelope indicates the magnitude of the Fourier transform, and the oscillations shown within the envelope represent the imaginary part of the Fourier transform.

(minor) contributions. This procedure was performed iteratively until an optimized fit (in  $k$  space and in  $r$  space) of the EXAFS function of the first-shell region was achieved. By fitting with  $k^1$  and  $k^3$  weighting in both  $k$  space and in  $r$  space, a unique set of coordination parameters for the low- $Z$  and high- $Z$  neighbors could be obtained.<sup>36</sup> Theoretically, the value of the relative energy,  $\Delta E$ , obtained from the EXAFS analysis of the data describes the difference in the absorption threshold energy between the sample and the reference compound. In the present analysis, the relative energy is used as an adjustable fitting parameter to compensate the uncertainty in the selection of the threshold energy of the EXAFS data characterizing the sample and the reference compound. Details of the method of data analysis are reported elsewhere.<sup>36-38</sup>

**Sample Prepared from  $\text{NH}_4\text{ReO}_4$  on  $\gamma$ -Al<sub>2</sub>O<sub>3</sub>.** EXAFS oscillations were observed for values of  $k$  up to  $14 \text{\AA}^{-1}$ , indicating that the data quality was very good. The  $\chi$  data were analyzed by isolating the first-shell region with a  $k^1$ -weighted Fourier transformation ( $\Delta k = 3.05$ – $13.98 \text{\AA}^{-1}$ ) and an inverse transformation with  $R_{\text{min}} = 1.27$  and  $R_{\text{max}} = 3.31 \text{\AA}$  (Figure 6).

A  $k^3$ -weighted Fourier transformation with Re–Re phase and amplitude corrections was carried out on these data ( $\Delta k = 3.72$ – $13.38 \text{\AA}^{-1}$ ) to identify the metal contributions. The imaginary part of the Fourier transform should peak positively at the radial distance corresponding to the Re–Re contribution.<sup>37</sup> The imaginary part was found to have a maximum and peaked positively at  $R = 2.74 \text{\AA}$ , which is consistent with the Re–Re distance in the bulk metal. This contribution was assigned to the Re–Re interaction in the sample. To obtain initial values for the coordination parameters of this Re–Re contribution, a one-shell analysis on the first-shell EXAFS data using a  $k^3$  weighting was

(36) Kampers, F. W. H. Ph.D. Dissertation, Eindhoven University of Technology, 1988.

(37) van Zon, J. B. A. D.; Koningsberger, D. C.; van't Blik, H. F.; Sayers, D. E. *J. Chem. Phys.* **1985**, *82*, 5742.

(38) van Zon, F. B. M.; Koningsberger, D. C.; Uh, Y. S.; Gates, B. C. *J. Am. Chem. Soc.* **1986**, *108*, 6254.

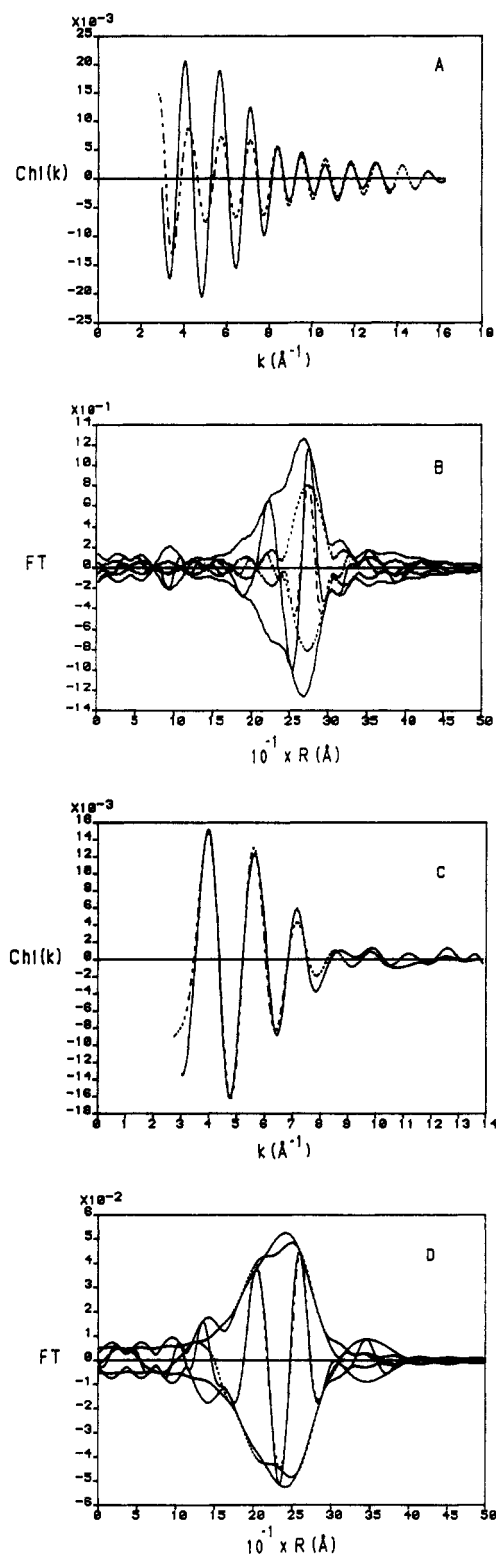


**Figure 6.** EXAFS spectra of a sample prepared by adsorption of  $\text{NH}_4\text{-ReO}_4$  on  $\gamma\text{-Al}_2\text{O}_3$  after reduction at  $450\text{ }^\circ\text{C}$ : (A) isolated EXAFS of the first coordination shell (solid line) and the calculated Re-Re EXAFS function (dashed line); (B) the  $k^1$ -weighted Fourier transform of the isolated first shell and the calculated Re-Re EXAFS function with Re-Re phase and amplitude correction; (C) the residual spectrum of the isolated EXAFS after the subtraction of the Re-Re EXAFS function (solid line) and the sum of the two calculated Re-O EXAFS functions (dashed line); (D) the Fourier transform of the residual spectrum and the sum of the two calculated Re-O EXAFS functions with  $k^1$  weighting, corrected for the Re-O phase shift.

performed ( $\Delta k = 3.72\text{--}13.38\text{ \AA}^{-1}$ ), emphasizing the metal contribution to the  $\chi$  data at high values of  $k$ . Figure 6A shows the calculated Re-Re contribution.

**TABLE IV: Structural Parameters Determined for the First Coordination Shell in the  $\text{H}_2$ -Treated Samples Prepared from  $\text{NH}_4\text{ReO}_4$  and  $\gamma\text{-Al}_2\text{O}_3$ <sup>a</sup>**

shell	$N$	$R, \text{\AA}$	$10^3\Delta\sigma^2, \text{\AA}^2$	$\Delta E, \text{eV}$
Re-O	1.9	2.07	10.7	-4.50
Re-O	1.5	2.60	0.58	-2.71
Re-Re	4.5	2.74	2.0	-0.98

<sup>a</sup> $N$ , coordination number.  $R$ , coordination distance.  $\Delta\sigma^2$ , relative Debye-Waller factor.  $\Delta E$ , relative energy. Estimated precision:  $N$ ,  $\pm 20\%$ ;  $R$ ,  $\pm 0.02\text{ \AA}$ ;  $\Delta\sigma^2$ ,  $\pm 20\%$ .

To investigate the possible presence of backscatters in addition to those indicated by the principal Re-Re contribution, a Re-Re phase- and amplitude-corrected Fourier transformation was performed with a  $k^1$  weighting (making the Fourier transform sensitive to low- $Z$  backscatters). The use of a  $k^1$ -weighted Fourier transform that has been corrected for the metal-metal phase and backscattering amplitude of the metal-metal contribution in order to detect the presence of low- $Z$  backscatters (typified by the oxygen of the support) has been discussed in publications dealing with the metal-support interface in supported metal catalysts.<sup>36-39</sup> The Fourier transform shown in Figure 6B is asymmetric both in magnitude and in the imaginary part at the low- $r$  side of the Re-Re peak located at  $2.74\text{ \AA}$ . This result indicates the presence of additional backscatters, since a proper phase and amplitude correction for the Re-Re contribution would result in a symmetric Fourier transform if no other contributions were present. The Re-Re EXAFS function calculated with the first-guess parameters was subtracted from the isolated first-shell EXAFS data. A  $k^1$ -weighted Fourier transform with a Re-O phase correction was applied to the residual spectrum. The imaginary part of the Fourier transform was found to peak positively at ca.  $2.0$  and  $2.6\text{ \AA}$ .

This result implies that Re interacted with low- $Z$  backscatters, such as oxygen, at two different radial distances. Since the precursor used was free of carbon, and since the short distance is in the range characteristic of bulk Re oxide while the long distance is similar to that reported for the metal-oxygen (M-O) ( $M = \text{Ir, Rh, Pt}$ ) distances characterizing the metal-support interfaces of highly dispersed supported metals on metal oxides in the presence of hydrogen,<sup>10,37,39</sup> the two low- $Z$  contributions are assigned to Re-O contributions. Coordination parameters for the two Re-O shells were determined and the two calculated Re-O functions subtracted from the first-shell experimental result. Now a better Re-Re contribution could be determined from the new residual spectrum. This procedure was repeated iteratively until good agreement was obtained between the experimental and the calculated first-shell results.

Further optimization was done on the first-shell data by fitting them with three contributions (two Re-O's and a Re-Re). This approach to EXAFS data analysis (combining fitting in  $k$  space and employment of the difference file technique) maximizes the likelihood of correct identification of the various EXAFS contributions and minimizes the possibility of misinterpretation resulting from trapping in local minima in the data fitting. The results of different steps in the analysis are shown in Figure 6. The final results of the EXAFS analysis in  $k$  space and in  $r$  space are shown in Figure 7, and the coordination parameters obtained are presented in Table IV.

*Sample Prepared by Adsorption of  $[\text{H}_3\text{Re}_3(\text{CO})_{12}]$  on  $\gamma\text{-Al}_2\text{O}_3$ .* The first-shell region was isolated by applying a  $k^1$ -weighted Fourier transformation ( $\Delta k = 3.05\text{--}10\text{ \AA}^{-1}$ ) to the EXAFS data and an inverse transformation with  $R_{\text{min}} = 1.02$  and  $R_{\text{max}} = 3.88\text{ \AA}$  (Figure 8A). The analysis procedure for the EXAFS data characterizing the sample prepared from  $[\text{H}_3\text{Re}_3(\text{CO})_{12}]$  on alumina treated in hydrogen at  $400\text{ }^\circ\text{C}$  was similar to that mentioned in the preceding section. An approximate Re-Re contribution was derived from the first-shell data. A  $\chi$  function was calculated on the basis of the Re-Re reference and subtracted

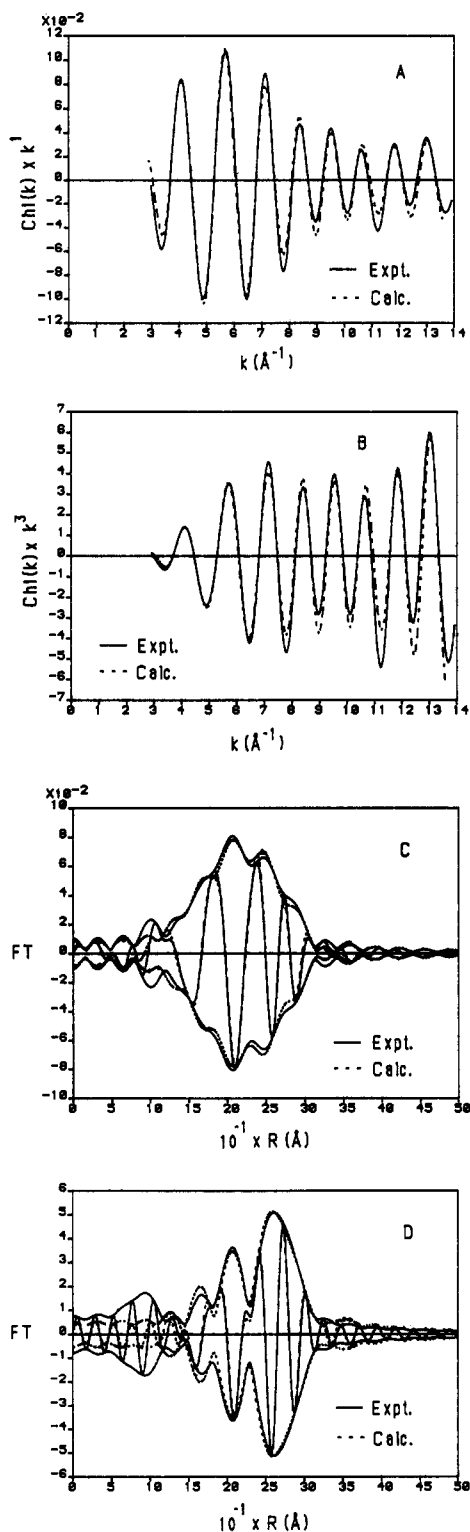


**Figure 7.** Analysis of EXAFS spectra characterizing a sample prepared by adsorption of  $\text{NH}_4\text{ReO}_4$  on  $\gamma\text{-Al}_2\text{O}_3$  after reduction at  $450^\circ\text{C}$ : isolated EXAFS of the first coordination shell and the sum of the calculated Re-O and Re-Re EXAFS functions (A) with  $k^1$  weighting and (B) with  $k^3$  weighting; Fourier transforms of the first coordination shell and the sum of the calculated Re-O and Re-Re EXAFS functions (C) with  $k^1$  weighting and (D) with  $k^3$  weighting.

from the data (Figure 8C). A  $k^1$ -weighted Fourier transformation with a Re-O phase correction was carried out on the residual spectrum. The imaginary part of the Fourier transform was found to peak positively, at two radial positions, indicating that the residual contribution consists of two low-Z backscatters (Figure 8D) such as oxygen (or possibly carbon). The EXAFS result is therefore interpreted as an indication of two Re-O contributions and one Re-Re contribution in the first-shell-region.

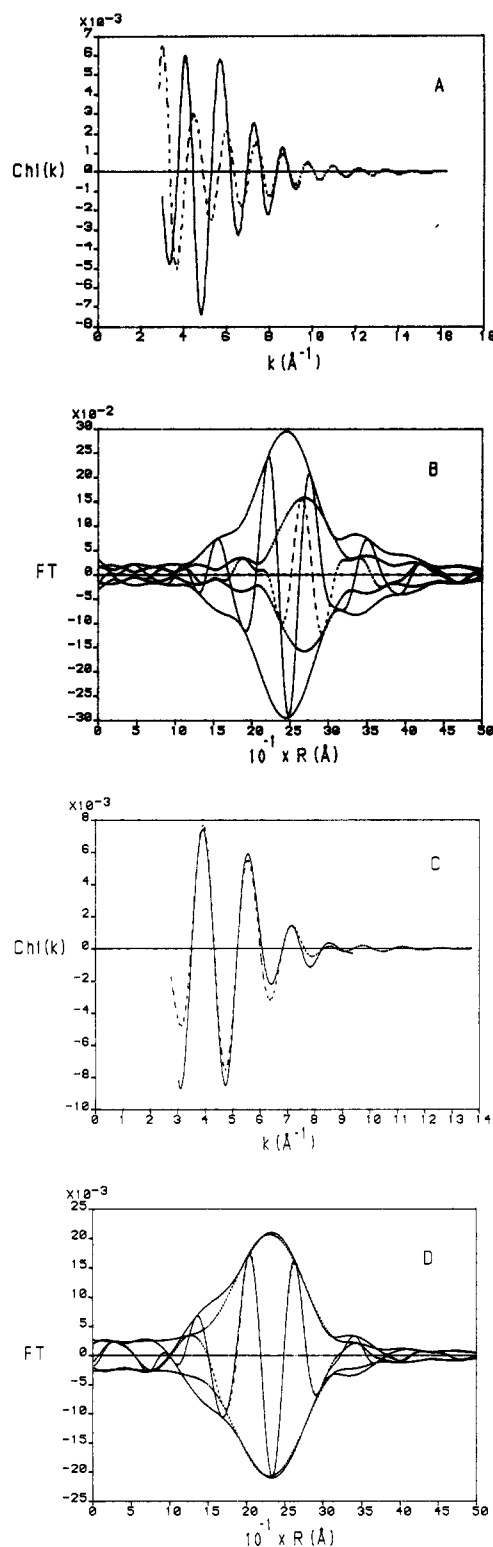


**Figure 8.** EXAFS spectra of a sample prepared by adsorption of  $[\text{H}_3\text{-Re}_3(\text{CO})_{12}]$  on  $\gamma\text{-Al}_2\text{O}_3$  after reduction at  $450^\circ\text{C}$ : (A) isolated EXAFS of the first coordination shell and the calculated Re-Re EXAFS function (solid line) and the calculated Re-O EXAFS function (dashed line); (B) the  $k^1$ -weighted Fourier transform of the isolated first shell and the calculated Re-Re EXAFS function with Re-Re phase and amplitude correction; (C) the residual spectrum of the isolated EXAFS after the subtraction of the Re-Re EXAFS function (solid line) and the sum of the two calculated Re-O EXAFS functions (dashed line); (D) Fourier transform of the residual spectrum and the sum of the two calculated Re-O EXAFS functions with  $k^1$  weighting, corrected for Re-O phase shift.

Recursive iterations were performed until there was a good agreement between the sum of the Re-O and Re-Re contributions and the first-shell data in  $k$  space and in  $r$  space (Figure 9). The coordination parameters are summarized in Table V.

**TABLE V: Structural Parameters Determined for the First Coordination Shell in the H<sub>2</sub>-Treated Sample Prepared from [H<sub>3</sub>Re<sub>3</sub>(CO)<sub>12</sub>] and  $\gamma$ -Al<sub>2</sub>O<sub>3</sub><sup>a</sup>**

shell	<i>N</i>	<i>R</i> , Å	10 <sup>3</sup> Δσ <sup>2</sup> , Å <sup>2</sup>	Δ <i>E</i> , eV
Re–O	0.7	2.05	9.7	–1.38
Re–O	1.0	2.58	6.6	2.13
Re–Re	2.0	2.67	8.6	–3.04

<sup>a</sup>*N*, coordination number. *R*, coordination distance. Δσ<sup>2</sup>, relative Debye–Waller factor. Δ*E*, relative energy. Estimated precision: *N*, ±20%; *R*, ±0.02Å; Δσ<sup>2</sup>, ±20%.

To demonstrate the reliability of the coordination parameters, the sum of the calculated Re–O and Re–Re contributions was Fourier transformed and compared with the first-shell data in *r* space (Figure 9). The agreement is good.

### Discussion

**Sample Prepared from NH<sub>4</sub>ReO<sub>4</sub>.** The short Re–O distance (*R* = 2.07 Å) obtained from the EXAFS analysis suggests that a fraction of the Re species remained oxidized after treatment of the sample in hydrogen at 450 °C. This result is consistent with the oxophilic character of Re; usually a hydrogen treatment temperature greater than 500 °C is needed to achieve reduction to the metallic state. Temperature-programmed reduction (TPR) data characterizing this sample, which had previously been dried at 500 °C in He, indicated a maximum rate of reduction at 438 °C.<sup>40</sup> The reduction was incomplete even after the sample had been held at 500 °C in hydrogen for 4 h.

The X-ray absorption edge data characterizing the sample prepared from NH<sub>4</sub>ReO<sub>4</sub> (Figure 3) show that the intensity of the L<sub>III</sub> absorption edge is similar to that of ReO<sub>2</sub>. This result can be reconciled with the TPR data only if the Re had been present in a range of oxidation states. Therefore, we infer that the sample consisted of a mixture of reduced and oxidized Re species after treatment in hydrogen.

The short Re–O distance is longer than that found in perhenate, [ReO<sub>4</sub>]<sup>–</sup> (*R*<sub>Re–O</sub> = 1.74 Å), but it is similar to one of the Re–O distances (*R*<sub>Re–O</sub> = 2.05 or 2.08 Å) characteristic of Re<sub>2</sub>O<sub>7</sub>.<sup>41</sup> The relatively large Debye–Waller factor (0.0107 Å<sup>2</sup>) observed for the supported Re sample may be interpreted as an indication of a distribution of Re–O distances, such as occurs in Re<sub>2</sub>O<sub>7</sub> (the range of Re–O distances being 1.65 to 2.16 Å). The Re–O distance of 2.07 Å is only an average. The results are consistent with the suggestion that a Re oxide phase was present on the support surface.

The Re–O distance at 2.60 Å is suggested to be associated with an interface between particles of Re metal and the  $\gamma$ -Al<sub>2</sub>O<sub>3</sub> support. The average Re–O coordination number corresponding to this distance is 1.5. Metal–oxygen distances in the range of 2.55–2.70 Å have been determined by EXAFS spectroscopy for various metals dispersed on metal oxide supports in the presence of hydrogen, including Ir,<sup>10</sup> Rh,<sup>37</sup> Pt,<sup>39</sup> and Re.<sup>22</sup> These relatively long metal–oxygen distances have been proposed to the interaction of reduced metal with hydroxyl groups of the metal oxide support.<sup>42</sup>

The Re–Re distance was found to be 2.74 Å, which is the value characteristic of bulk Re metal. The Re–Re coordination number corresponding to this distance was determined to be 4.5. Since the fraction of Re that had been reduced after 4 h at 450 °C in hydrogen is not known, this Re–Re coordination number is only an average that does not represent the actual coordination number of the Re particles. The coordination number calculated from the data is an average over all the Re atoms in the sample

$$N_{\text{red.}} = (N_{\text{red.}})_{\text{EXAFS}}/f \quad (1)$$

where *N*<sub>red.</sub> is the Re–Re coordination number of the reduced (metallic) Re particle and *f* is the fraction of Re in the metallic

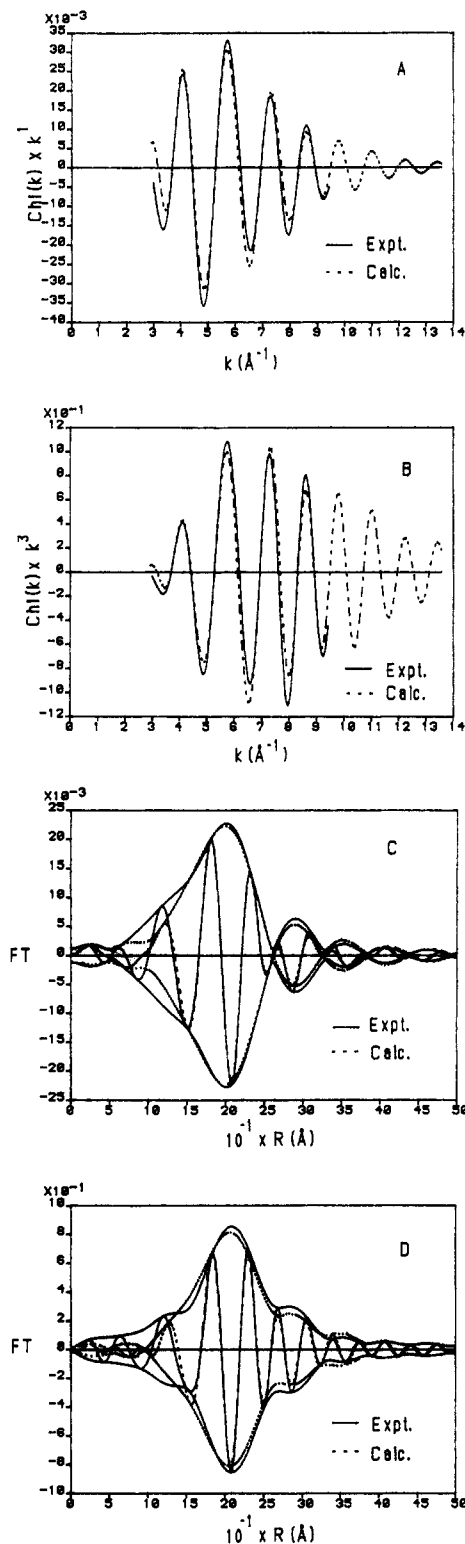


**Figure 9.** Analysis of EXAFS spectra characterizing a sample prepared by adsorption of [H<sub>3</sub>Re<sub>3</sub>(CO)<sub>12</sub>] on  $\gamma$ -Al<sub>2</sub>O<sub>3</sub> after reduction at 400 °C: isolated EXAFS of the first coordination shell and the sum of the calculated Re–O and Re–Re EXAFS functions (A) with *k*<sup>1</sup> weighting and (B) with *k*<sup>3</sup> weighting; Fourier transforms of the first coordination shell and the sum of the calculated Re–O and Re–Re EXAFS functions (C) with *k*<sup>1</sup> weighting and (D) with *k*<sup>3</sup> weighting.

phase. Therefore, the Re–Re coordination number can be used only as a lower limit to estimate the metal particle size. This lower limit of the average particle diameter is estimated to be ca. 10 Å, assuming on average a hemispherical 15-atom particle with an average coordination number of 4.73.

In summary, an alumina-supported Re sample prepared from NH<sub>4</sub>ReO<sub>4</sub> gave a mixture of surface species after treatment in

(40) Fung, A. S. Ph.D. Dissertation, University of Delaware, 1989.

(41) Krebs, B.; Müller, A.; Beyer, H. H. *Inorg. Chem.* **1969**, *8*, 436.

(42) Martens, J. H. Ph.D. Dissertation, Eindhoven University of Technology, 1988.

hydrogen at 450 °C. An oxidic phase was present with an average Re–O distance of 2.07 Å. Re particles with the characteristic bulk Re–Re distance of 2.74 Å were also observed. The presence of these two phases made it difficult to determine the average Re particle size.

**Sample Prepared from [H<sub>3</sub>Re<sub>3</sub>(CO)<sub>12</sub>].** Two types of Re–O contributions are indicated by EXAFS data characterizing the sample prepared from [H<sub>3</sub>Re<sub>3</sub>(CO)<sub>12</sub>]. The distances were found to be the same as those observed for the sample prepared from NH<sub>4</sub>ReO<sub>4</sub>, but with lower coordination numbers (0.7 and 1.0). The coordination number of 1.0 corresponding to the long Re–O contribution at 2.58 Å is lower than that corresponding to models representative of small metal particles on metal oxide surfaces (e.g., with the reduced metal atoms positioned at the threefold sites on the oxygen layer of an alumina support). The Re–Re coordination number was determined to be 2.0 (Table V), implying that, on average, Re was present in groups of only three atoms. But such highly dispersed Re would require a coordination number corresponding to the long Re–O contribution closer to three than to one (which was observed) in order to satisfy the coordination of the Re. Therefore, the data are modeled with a structure having two Re–O contributions.

These results provide evidence for a structural model consisting of small Re entities positioned on the alumina surface. The results of the XP spectroscopy and the X-ray absorption measurements indicate that the Re was cationic. The low coordination number of the Re–O contributions at 2.05 Å suggests that each Re was positioned atop an oxygen atom of the support.

Moreover, the Re–Re distance was found to be 2.67 Å, which is about 0.07 Å shorter than the bulk metal distance. Metal–metal bond distances less than those in the bulk metal have been observed for Fe dimers isolated in inert matrices at low temperature<sup>43</sup> and for Ru surface species derived from [Ru<sub>3</sub>(CO)<sub>12</sub>] adsorbed on  $\gamma$ -Al<sub>2</sub>O<sub>3</sub>.<sup>44</sup> A short Re–Re distance has also been observed in a dinuclear Re(II) complex with terminal oxo ligands, [Re<sub>2</sub>O<sub>2</sub>(MeC≡CMe)<sub>4</sub>];<sup>45</sup> Re cations are bonded to each other with a distance of 2.686 Å, and each Re has a short multiple terminal bond to oxygen in the molecular complex.

The Re–Re distance determined for the supported sample prepared from [H<sub>3</sub>Re<sub>3</sub>(CO)<sub>12</sub>] is close to the Ir–Ir distance determined for an alumina-supported sample prepared from [Ir<sub>4</sub>(CO)<sub>12</sub>].<sup>10</sup> The Ir particles thus formed were inferred to be monolayer rafts, with each Ir atom positioned at a threefold site on the stable  $\gamma$ -Al<sub>2</sub>O<sub>3</sub> [111] surface, which is the surface predominantly exposed in small  $\gamma$ -Al<sub>2</sub>O<sub>3</sub> particles.<sup>46–48</sup> The O–O distance in bulk  $\gamma$ -Al<sub>2</sub>O<sub>3</sub> has been determined to be 2.8 Å by electron diffraction measurements.<sup>46</sup> Surface reconstruction of the oxide support was proposed to occur at the metal–support interface, leading to O–O distances in the first two oxygen layers (2.68 Å) that are nearly equal to the first-shell Ir–Ir distance determined by EXAFS analysis. The shrinkage in the O–O distance to adapt to the Ir–Ir distance suggests that a certain degree of flexibility exists in the first two oxygen layers at the metal–support interface.

On the basis of (1) the derived average Re–Re distance in this work, (2) an assumption similar to that stated above concerning the O–O distance of a reconstructed alumina [111] surface, and (3) the low Re–O coordination number, a structural model is proposed, consisting of three Re atoms forming a raft lying atop the oxygens of the [111] face of the oxide support, with  $N_{\text{Re–Re}} = 2.0$  and  $R_{\text{Re–Re}} = 2.67$  Å (Figure 10). The short Re–O distance at 2.05 Å suggests that the Re atoms are tethered to surface oxygen atoms. The bonding may be similar to that in the complex [Re<sub>2</sub>O<sub>2</sub>(MeC≡CMe)<sub>4</sub>], for which the Re=O distance is 1.69 Å.<sup>45</sup>

(43) Purdum, H.; Montano, P. A.; Shenoy, G. K.; Morrison, T. *Phys. Rev. B* **1982**, *25*, 4412.

(44) Udagawa, Y.; Tohjik, K.; Lin, Z. Z.; Okuhara, T.; Misono, M. *J. Phys.* **1986**, *C8*, 249.

(45) Valencia, E.; Santarsiero, B. D.; Geib, S. J.; Rheingold, A. L.; Mayer, J. M. *J. Am. Chem. Soc.* **1987**, *109*, 6896.

(46) Lippens, B. C.; de Boer, J. H. *Acta Crystallog.* **1964**, *17*, 1312.

(47) Iijima, S. *Jpn. J. Appl. Phys.* **1984**, *23*, L347.

(48) Iijima, S. *Surf. Sci.* **1985**, *156*, 1003.

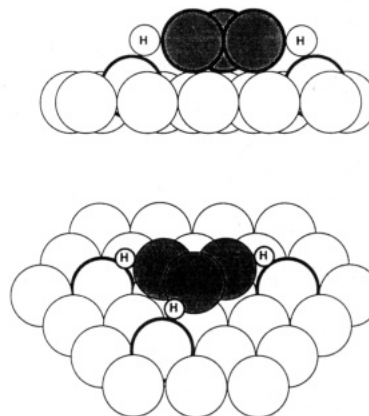


Figure 10. Structural model of a Re surface raft based on the coordination parameters obtained from EXAFS analysis.

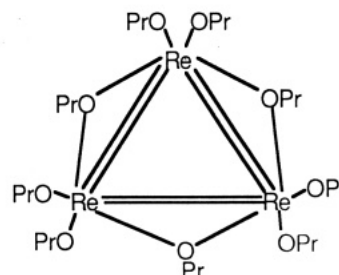


Figure 11. Proposed structure of [Re<sub>3</sub>( $\mu$ -O-i-Pr)<sub>3</sub>(O-i-Pr)<sub>6</sub>].<sup>51</sup>

The short distance between Re and the surface oxygen indicates a strong metal–support bond, corresponding to the cationic nature of Re. The Re–O contribution observed at 2.58 Å is suggested to correspond to Re interacting weakly with hydroxyl groups as additional surface ligands, probably formed during the treatment in hydrogen.

The implication of this structure is that the nuclearity of the precursor [H<sub>3</sub>Re<sub>3</sub>(CO)<sub>12</sub>] was retained as it was transformed on the surface. Evidently, the strength of the Re–O bonds was sufficient to anchor the metal to the support before substantial migration of rhenium occurred.

EXAFS data have also provided evidence of trinuclear ensembles of Re prepared from [H<sub>3</sub>Re<sub>3</sub>(CO)<sub>12</sub>] on MgO after treatment in helium at 250 °C.<sup>22</sup> However, a nonbonding average Re–Re distance of 3.94 Å was observed, and the Re retained some of its CO ligands (three CO's per Re). Evidently, in this example also, the strength of the Re–O bonds was sufficient for retention of nuclearity after cluster breakup on the surface.

The transformation of the alumina-supported sample prepared from [H<sub>3</sub>Re<sub>3</sub>(CO)<sub>12</sub>] prior to its conversion into the structure described here has been characterized by in situ infrared spectroscopy.<sup>40</sup> The initial surface species undergoes decarbonylation with cluster fragmentation, resulting in the formation of Re subcarbonyl species.<sup>21</sup> Further treatment in hydrogen at 400 °C leads to complete decarbonylation of the Re surface species. The decarbonylated Re species might have become coordinatively unsaturated and bonded to each other to form small rafts of, on average, three Re atoms on the  $\gamma$ -Al<sub>2</sub>O<sub>3</sub> surface. The presence of the long Re–O contribution, possibly indicative of the interaction of Re with hydroxyl groups, might be accounted for by the hydrogenation of the CO ligands of the Re subcarbonyl species during hydrogen treatment, leading to the formation of methane and water, with the latter reacting with the surface to form hydroxyl groups.<sup>49</sup>

**Metal Surface–Metal Cluster Analogy.** The model depicted in Figure 10 is based on the structural parameters determined in the EXAFS analysis. The structure is best described as a small cationic Re raft lying atop the oxygens of the metal oxide support. Similar small raftlike molecular structures are known and might

(49) Kirilin, P. S. Ph.D. Dissertation, University of Delaware, 1986.

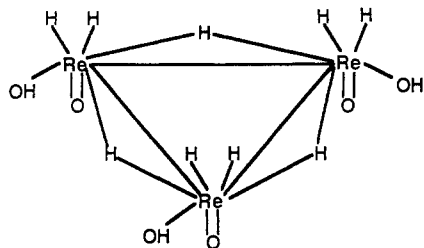


**Figure 12.** Structure of proposed Re surface species,  $[\text{Re}_3\text{O}_3(\mu\text{-H}_3)(\text{OH})_3\text{H}_6]$ .

be considered to be analogous, e.g.,  $[\text{W}_3\text{O}(\text{O-i-Pr})_{10}]$ ,<sup>50</sup> which incorporates trinuclear oxo-capped tungsten, and  $[\text{Re}_3(\mu\text{-O-i-Pr})_3(\text{O-i-Pr})_6]$ <sup>51</sup> (Figure 11). In the former complex, W is in a formal +4 oxidation state. Re has a formal oxidation state of +3 in the latter complex, with a Re–Re distance of 2.38 Å.<sup>51</sup> In the present investigation, the Re has also been shown to exist in a high-valent state, as determined by XPS and confirmed by the threshold resonance experiments. Each Re has four oxygen neighbors in the rhenium alkoxide, but only two average Re–O contributions were observed in the first shell of Re on the  $\text{Al}_2\text{O}_3$  surface. The difference in the bonding and structure may be caused by the differences of the oxygen-containing ligands in their ability to satisfy the coordination of Re; the inflexibility of the surface oxygens may restrict their bonding to Re relative to the alkoxide ligands.

The small number of Re–oxygen interactions at the surface and the smallness of the Re entities (indicated by the Re–O and Re–Re coordination numbers) suggest strong metal–metal bonding in the surface structure. Cotton<sup>52,53</sup> observed multiple metal–metal bonds in Mo, Cr, W, and Re complexes, which are usually dinuclear, with the metal in a low oxidation state. The metals are bonded together either by quadruple or triple bonds with distances of about 2.3 Å. In the sample prepared by adsorbing  $[\text{H}_3\text{Re}_3(\text{CO})_{12}]$  on  $\gamma\text{-Al}_2\text{O}_3$  (after reduction at 400 °C), the Re–Re distance was found to be 2.67 Å, which is greater than the distances characterizing the quadruple and triple bonds but shorter than the distance in metallic Re (2.74 Å). The Re–Re distance suggests an intermediate bond order (roughly 1.5<sup>54</sup>), which allows the Re to coordinate with other ligands provided by the surface. The bonding and structure of the surface species may be roughly comparable to those in the  $\text{M}_3\text{L}_3\text{X}_9$  type cluster.<sup>55</sup>

If the surface structure of the trinuclear Re ensemble is assumed to be analogous to that of the  $\text{M}_3\text{L}_3\text{X}_9$  cluster, three of the axial

ligands on the same face can be the oxo ligands derived from the support. The interaction between surface oxo groups and supported metals has also been observed in other samples. The equatorial positions are occupied by the neighboring Re atoms in the ensembles. The atop axial and bridging sites may be assumed to be occupied by hydride ligands originating from  $\text{H}_2$  dissociation. The hydride cannot be detected by the X-ray methods. Alternatively, the presence of an overlayer of carbon might also be postulated to assist in stabilizing the surface raft structure.

The hydride structure could be formed as  $\text{H}_2$  is oxidatively added to low-valent Re during the hydrogen treatment at high temperatures, leading to an increase in the oxidation state of Re. The plausibility of this suggestion is indicated by the existence of a high-valent Re hydride complex,  $[\text{ReH}_9]^{2-}$ .<sup>56</sup> However, the low coordination number of low-Z backscatters characterized by EXAFS spectroscopy is not consistent with this proposal. A trinuclear Re cluster with a formula of  $[\text{Re}_3\text{O}_3(\mu\text{-H}_3)(\text{OH})_3\text{H}_6]$  (Figure 12) may have a total of 54 electrons, if each oxo ligand donates four electrons. However, one must take into account the binding of the oxygens with the support. If these Re–oxygen support bonds account for a total of only six electrons, the total number of electrons in the trinuclear Re cluster will be 48, with each Re having 16 electrons. Quantum mechanical calculations may help to elucidate how small raftlike structures exist on the surface and how they compare with organometallic analogues.

### Conclusions

1. The sample made from  $\text{NH}_4\text{ReO}_4$  consists of a mixture of rhenium oxide and highly dispersed rhenium metal particles on the  $\gamma\text{-Al}_2\text{O}_3$  surface.

2. The sample prepared from  $[\text{H}_3\text{Re}_3(\text{CO})_{12}]$ , in contrast, consists of raftlike trirhenium structures on the  $\gamma\text{-Al}_2\text{O}_3$  surface. The average Re–Re distance in the rafts is 2.67 Å. There are two Re–O distances, 2.05 and 2.58 Å. The structure is modeled as  $\text{Re}_3$  entities atop oxygen atoms of the [111] surface of  $\gamma\text{-Al}_2\text{O}_3$ , accounting for the shorter Re–O distance. Interactions with surface hydroxyl groups are postulated to account for the longer Re–O distance. The Re–Re bonds in the rafts are shorter than those in Re metal (2.74 Å), and the bond order is roughly 1.5.

*Acknowledgment.* We thank S. D. Maloney and C. J. Papile for help with the EXAFS experiments and K. M. Sanchez and G. C. A. Schuit for helpful discussions. The EXAFS experiments were performed at beamline X-11-A at the National Synchrotron Light Source at Brookhaven National Laboratory, and the Synchrotron Radiation source at the Daresbury Laboratory (U.K.). We thank the synchrotron staffs for their help. This research was supported by the U.S. Department of Energy, Office of Energy Research, Office of Basic Energy Sciences (Contract FG02-87ER13790). Beamline X-11-A at the National Synchrotron Light source is supported by the U.S. Department of Energy.

(50) Chisholm, M. H.; Folting, K.; Huffman, J. C.; Kober, E. M. *Inorg. Chem.* **1985**, *24*, 241.

(51) Hoffman, D. M.; Lappas, D.; Wiedra, D. A. *J. Am. Chem. Soc.* **1989**, *111*, 1531.

(52) Cotton, F. A. *Acc. Chem. Res.* **1978**, *11*, 225.

(53) Cotton, F. A. *Acc. Chem. Res.* **1978**, *11*, 356.

(54) Kožmin, P. A.; Surazhskaya, M. D. *Koord. Khim.* **1980**, *6*(5), 309.

(55) Cotton, F. A.; Wilkinson, G. *Advanced Inorganic Chemistry*, 4th ed.; Wiley: New York, 1980; p 1096.

(56) Ginsberg, A. P.; Sprinkle, C. R. *Inorg. Chem.* **1969**, *8*, 2212.